Supporting Information

Molecular Cobalt Catalysts for O_2 Reduction to H_2O_2: Benchmarking Catalyst Performance via Rate–Overpotential Correlations

Yu-Heng Wang,[‡] Biswajit Mondal, and Shannon S. Stahl*

Department of Chemistry, University of Wisconsin–Madison, Madison, Wisconsin 53706, USA

*Corresponding Author: stahl@chem.wisc.edu.

[‡]Current Address: Y. H. W.: Department of Chemistry, National Tsing Hua University, Hsinchu 30013, Taiwan.

Table of Contents

I. General considerations

All commercially available reagents and solvents were used as received, except where otherwise noted. Perchloric acid (70%) was obtained from Sigma Aldrich. UV-Vis spectra were recorded on an Agilent Cary 60 spectrometer.

II. OCP measurements of E_{H^+/H_2} using literature conditions

A. Open-circuit potential (OCP) measurements for E_{H^+/H_2} with different buffered conditions. The H^+/H_2 potential in organic media can be determined through open-circuit potential measurements at a Pt electrode using a recently reported protocol.[1] The H^+/H_2 potentials were measured for DMF with various buffered conditions under 1 atm H_2 (local atmospheric pressure of 752 mm Hg, correction to 1 atm < 1 mV). All DMF solutions were containing 0.1 M $[NBu_4][ClO_4]$ as supporting electrolyte. These conditions were chosen to give media that have stable, well-defined thermodynamics for the H^+/H_2 equilibria. Stable open-circuit potentials of H^+/H_2 (E_{H^+/H_2}) were observed, and E_{H^+/H_2} were referenced to $Fc^{*+/0}$ by adding decamethylferrocene and performing CV at a second, glassy carbon working electrode in the same solution (Figure S1).

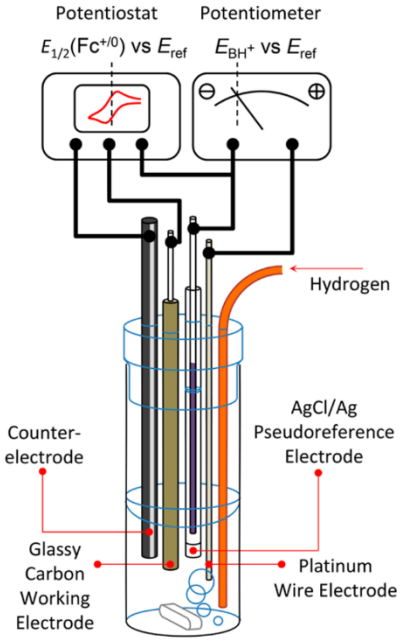

Figure S1. Schematic of the four-electrode cell configuration used for open circuit potential (OCP) measurements.[1] The reduction potential of H^+/H_2 was measured for DMF solutions with various buffered conditions under 1 atm H_2. All DMF solutions were containing 0.1 M $[NBu_4ClO_4]$ as supporting electrolyte (Figure S1 is reproduced from ref. 1; copyright 2013 American Chemical Society.)

B. Homogeneous O_2 reduction catalyzed by monomeric Co complexes in the literature were conducted in aqueous or organic solutions. To estimate the thermodynamic reduction potentials of O_2/H_2O_2 (E_{O_2/H_2O_2}) of that ORR conducted in organic solutions, the OCP measurements of E_{H^+/H_2} were performed to estimate E_{O_2/H_2O_2} under different reaction conditions (Figures S2 and S3). In additions, corresponding buffered conditions are used for all OCP measurements of E_{H^+/H_2}. Buffered conditions are used because the presence of "buffer" ensures that there are only negligible changes in the proton concentration during the OCP measurements of E_{H^+/H_2}. All reported E_{H^+/H_2} are relative to the $Fc^{*+/0}$.

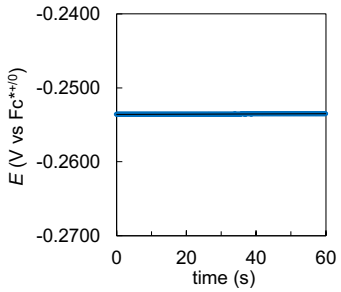

Figure S2. The black traces show the average OCP of E_{H^+/H_2} with 10 mM $HClO_4$ in DMF under 1 atm H_2. $E_{H^+/H_2} \approx -0.25$ V vs. $Fc^{*+/0}$. Supporting electrolyte: 0.1 M [NBu_4ClO_4].

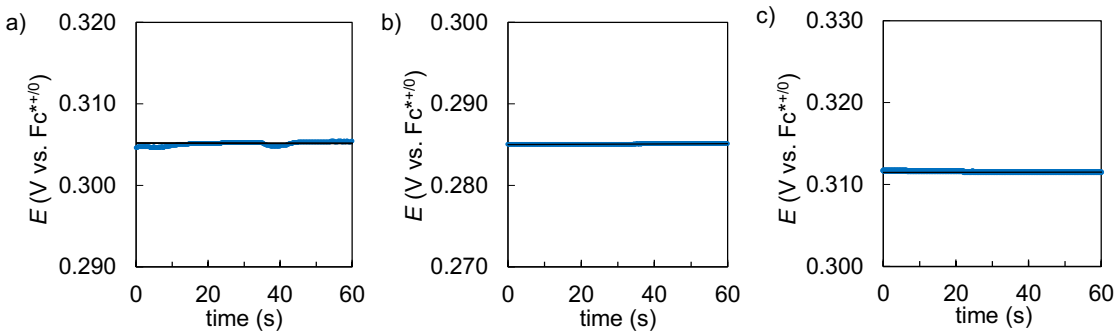

Figure S3. The OCP measurements of E_{H^+/H_2} under 1 atm H_2 for different conditions: (a) 20 mM $HClO_4$ in MeCN;[2] (b) 20 mM each of $HClO_4$ in PhCN;[3,4] (c) 50 mM $HClO_4$ in PhCN.[5,6] Supporting electrolyte: 0.1 M [NBu_4ClO_4].

III. Estimation of E_{O_2/H_2O_2} based on the literature conditions

A. Estimation of E_{O_2/H_2O_2} based on E_{H^+/H_2} measured by OCP.[7]

The reduction potential for O_2/H_2O_2 in DMF may be estimated using i) the standard aqueous cell potential for $O_2 + H_2 \rightarrow H_2O_2$, ii) the measurement of the open circuit potential (OCP) for H^+/H_2 (E_{H^+/H_2}) (cf. Figure S2), and iii) the Gibbs free energy to transfer H_2O_2 from H_2O to DMF.[8,9] For instance, E_{O_2/H_2O_2} for the DMF solution in the presence of 10 mM each of $HClO_4$ and $[NBu_4][ClO_4]$ is calculated by the following equations:

i)	$O_{2(g)} + H_{2(g)} \rightleftharpoons H_2O_{2(aq)}$	$E°_{O_2/H_2O_{2(aq)}}$	= 0.68 V vs $E_{H^+/H_{2(aq)}}$
ii)	$2\ H^+_{(DMF)} + 2\ e^-_{(V\ vs\ Fc^{*+/0})} \rightleftharpoons H_{2(g)}$	$E_{H^+/H_{2(DMF)}}$	= –0.25 V vs $Fc^{*+/0}$
iii)	$H_2O_{2(aq)} \rightleftharpoons H_2O_{2(DMF)}$	$\Delta G_{H_2O_{2(aq \rightarrow DMF)}}$	= < 1 kcal/mol
$O_{2(g)} + 2\ e^-_{(V\ vs\ Fc^{*+/0})} + 2\ H^+_{(DMF)} \rightleftharpoons H_2O_{2(DMF)}$		**$E_{O_2/H_2O_{2(DMF)}}$ = 0.43 V vs $Fc^{*+/0}$**	

Table S1. A summary of reduction potentials of H^+/H_2 and O_2/H_2O_2 under organic conditions in the literature. All potentials are relative to the $Fc^{*+/0}$.

	DMF, 10 mM $HClO_4$[a]	MeCN, 20 mM $HClO_4$	PhCN, 20 mM $HClO_4$	PhCN, 50 mM $HClO_4$
$E_{H^+/H2}$	-0.25 V	0.31 V	0.29 V	0.31 V
$E_{O2/H2O2}$[b]	0.43 V	0.99 V	0.97 V	0.99 V

[a]Reaction condition for this study. [b]At the standard-state condition of 1 M H_2O_2, $E_{O_2/H_2O_2} = E_{H^+/H_2} + 0.68$ V.

B. A thermodynamic reduction potential of E_{O_2/H_2O_2} under standard state conditions

The oxygen reduction catalyzed by **1**–**8** were conducted in the presence of 100 μM urea·H_2O_2 to establish a stable thermodynamic reference state for the effective overpotential. Because previous studies of catalytic ORR typically do not include a background concentration of H_2O_2 in the reaction medium, we elected not to use this reference state in the effective overpotentials reported here to ensure that all catalysts were treated the same way. Hence, the effective overpotentials were calculated by assuming the reactions were performed under standard-state conditions for the entire study (i.e., 1 M H_2O_2). At standard-state conditions, the thermodynamic reduction potential of E_{O_2/H_2O_2} under our catalytic conditions is calculated to be 0.43 V.

IV. Electrochemical experiments

A. General considerations for cyclic voltammetry (CV).

All CV experiments were performed with a CH Instrument 600E Potentiostat at room temperature. The supporting electrolyte for all electrochemical experiments was 0.1 M tetrabutylammonium perchlorate ($[NBu_4][ClO_4]$). The three-electrode setup for all cyclic voltammogram measurements included a glassy carbon (GC) working electrode (3.0 mm diameter), a platinum (Pt) wire counter electrode, and a 0.01 M $Ag/AgNO_3$ non-aqueous reference electrode.

B. Cyclic Voltammograms of 1–8 in DMF.

1. The half-wave potentials of Co(por) complexes **1**–**8** ($E_{1/2}(Co^{III/II})$) were recorded both in the absence and presence of 10 mM $HClO_4$. Half-wave potentials were recorded under buffered conditions because the catalytic rates of O_2 reduction were measured under buffered conditions (*vide infra*). Therefore, the $E_{1/2}(Co^{III/II})$ used to calculate the effective overpotentials in this study (cf. eq 3 in the main manuscript)

reflects the actual $E_{1/2}(Co^{III/II})$ under catalytic conditions, which ensures effective overpotential are calculated correctly.

2. Buffered conditions are used in the catalytic reaction because protons are consumed in the catalytic reaction, and the presence of "buffer" ensures that there are only negligible changes in the proton concentration (cf. Section V).

Chart S1. Molecular Co(por) complexes **1–8** in this study

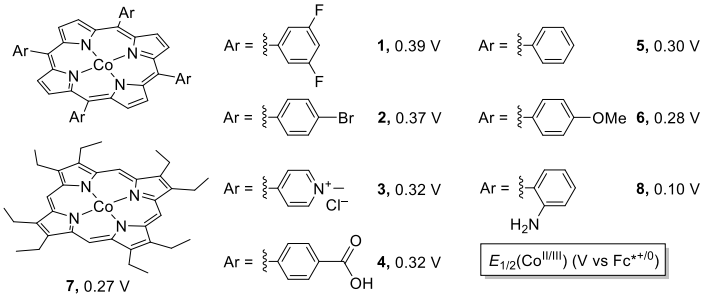

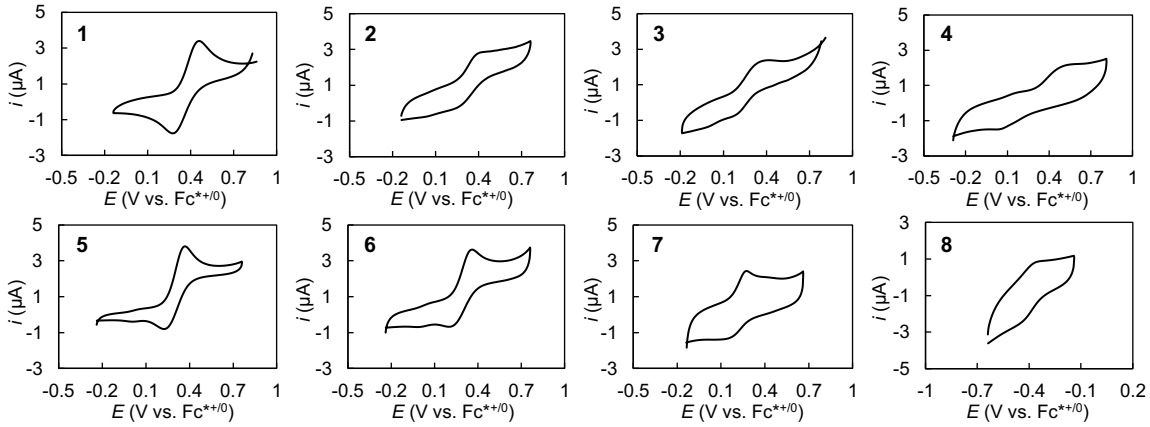

Figure S4. Cyclic voltammograms of 1 mM **1–8** in DMF solutions. All CVs were recorded under 1 atm N_2 at the scan rate of 10 mV/s, and all $E_{1/2}(Co^{III/II})$ are relative to the $Fc^{*+/0}$.

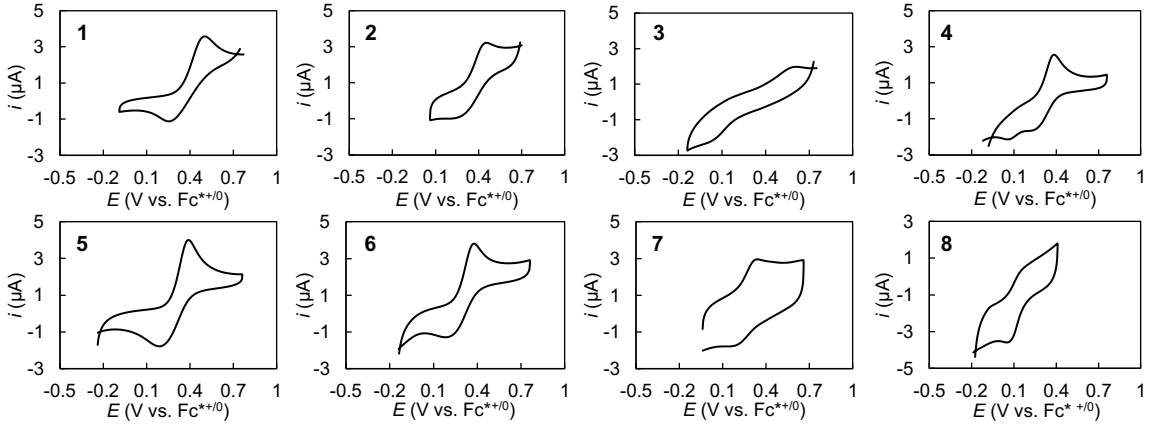

Figure S5. Cyclic voltammograms of 1 mM **1–8** in DMF solutions containing of 10 mM $HClO_4$. All CVs were recorded under 1 atm N_2 at the scan rate of 10 mV/s, and all $E_{1/2}(Co^{III/II})$ are relative to the $Fc^{*+/0}$.

Table S2. A summary of $E_{1/2}(Co^{III/II})$ of **1–8** in the absence and presence of 10 mM each of $HClO_4$ and $[NBu_4][ClO_4]$. All $E_{1/2}(Co^{III/II})$ are relative to the $Fc^{*+/0}$.

Conditions \ $E_{1/2}$ (V)	**1**	**2**	**3**	**4**	**5**	**6**	**7**	**8**
0 mM $HClO_4$/$[NBu_4][ClO_4]$	0.40	0.38	0.29	0.29	0.30	0.29	0.22	-0.42
10 mM $HClO_4$/$[NBu_4][ClO_4]$	0.39	0.37	0.32	0.32	0.30	0.28	0.26	0.10

Table S3. A summary of effective overpotentials (η_{eff}, V) for the O_2 reduction catalyzed by **1–8**.[a,b]

Co(por)	**1**	**2**	**3**	**4**	**5**	**6**	**7**	**8**
η_{eff} (V) at standard state condition[c]	0.04	0.06	0.11	0.11	0.13	0.15	0.17	0.33

[a] Buffered conditions: 10 mM each of $HClO_4$ and $[NBu_4][ClO_4]$. [b] $\eta_{eff} = E_{O_2/H_2O_2} - E_{1/2}(Co^{III/II})$, E_{O_2/H_2O_2} = 0.43 V vs. $Fc^{*+/0}$ (section III). [c]The effective overpotentials at standard state conditions were used for Figures 2, 5 and 6 in the main manuscript.

V. Turnover frequencies of ORR catalyzed by 1–8

A. General considerations for kinetic studies of O_2 reduction catalyzed by 1–8.

1. Catalytic O_2 reduction was followed by UV-visible spectroscopy at 780 nm, where an increase in absorption is observed due to the formation of Fc^{*+}.[10] A background concentration of 100 μM urea·H_2O_2 was added each of the reaction mixture to establish a stable thermodynamic reference state. This 10^4-fold difference in $[H_2O_2]$ compared to the standard state conditions (1 M H_2O_2) formally would correspond to a 120 mV Nernstian shift in the thermodynamic O_2/H_2O_2 potential (cf. Section III). Control experiments showed that neither the presence of urea nor the presence of urea·H_2O_2 in the reaction mixture influences the reaction rate.

2. Each catalytic experiment was conducted under buffered conditions. Because protons are consumed in the catalytic reduction of O_2, and the presence of "buffer" ensures that there are not large changes in the proton concentration during the course of the catalytic reaction. In addition, buffered conditions are crucial to establish a stable thermodynamic reduction potential for O_2/H_2O_2 under the reaction conditions (cf. Sections I–II).

B. Experimental protocol for catalytic O_2 to H_2O_2 by 1–8.

A 2.7 mL DMF solution of 1.1 mM Fc*, 110 μM urea·H_2O_2, and 11 mM $[NBu_4][ClO_4]$ was vigorously sparged with O_2 for 3 minutes to prepare the O_2-saturated solution. A 0.3 mL N_2-saturated DMF solution containing the cobalt complex being investigated (**1–8**, 0.1–100 μM) and 100 mM $HClO_4$ was rapidly injected into the O_2-saturated DMF solution. The reaction mixture was then vigorously shaken for 20 sec and the absorbance was monitored at 780 nm by UV-visible spectroscopy. The final concentration of each of the components in the reaction mixture is as follows: 1 mM Fc*, 0.01–10 μM **1–8**, 10 mM each of $HClO_4$ and $[NBu_4][ClO_4]$, 100 μM urea·H_2O_2, and 4.5 mM O_2.[11]

C. Calculations of turnover frequencies (TOFs).

Background O_2 reduction by Fc* was observed in the absence of **1–8** under the experimental conditions (Figure S6, gray traces),[12] and the rate of this background reaction was subtracted from the initial rates obtained from the reactions conducted in the presence of catalysts (Figure S7). Initial rates, in units of $mM \cdot s^{-1}$, were obtained by fitting UV-visible time-course data with linear regression during the first ~5% of the reaction, as shown by insets in the plots below (Figure S7). The turnover frequencies (TOFs, s^{-1}) were

then determined by dividing the number of electron transferred (to account for the conversion of O_2 to H_2O_2 or H_2O on the basis of consumption of single-electron reductant, Fc*) and the catalyst concentration (TOF $(s^{-1}) = \frac{\Delta[Fc^*]/2}{[Co]\times time}$).

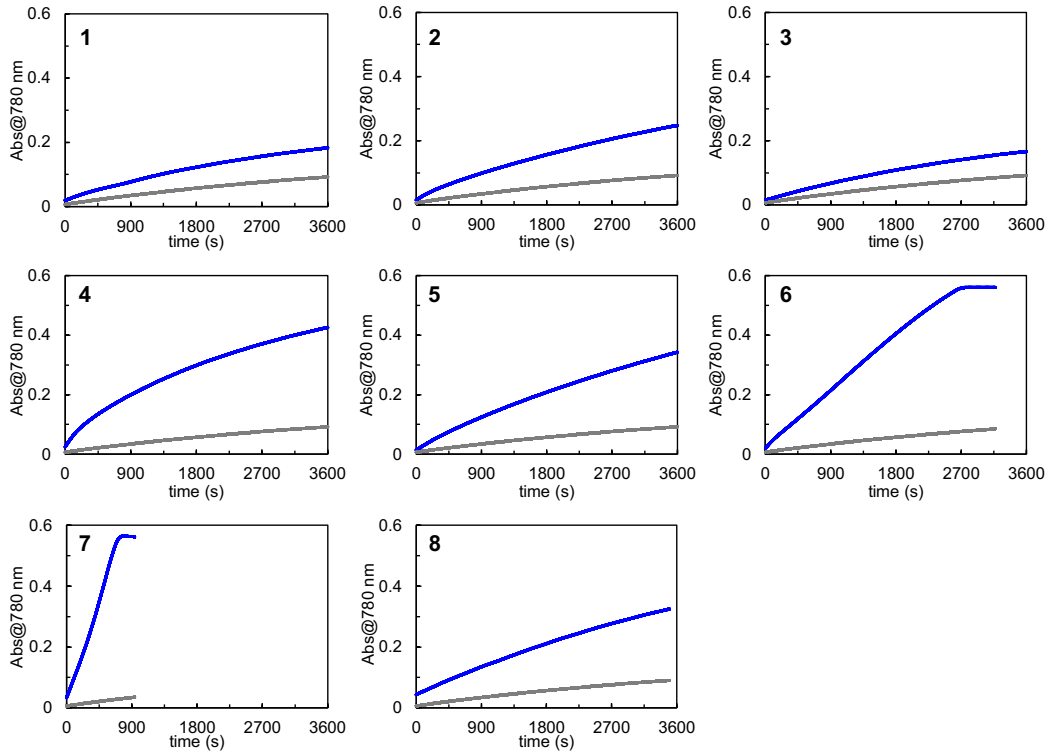

Figure S6. UV-visible time-course raw data for the catalytic O_2 reduction**.** Blue trace: the formation of Fc^{*+} due to the catalytic O_2 reduction and the background O_2 reduction by Fc*; gray trace: the formation of Fc^{*+} due to the background O_2 reduction by Fc* (in the absence of Co catalysts). Concentration of Co complexes **1–8** for each study: **1**, 10 μM; **2**, 10 μM; **3**, 1 μM; **4**, 10 μM; **5**, 2 μM; **6**, 2 μM; **7**, 2.5 μM; **8**, 0.01 μM.

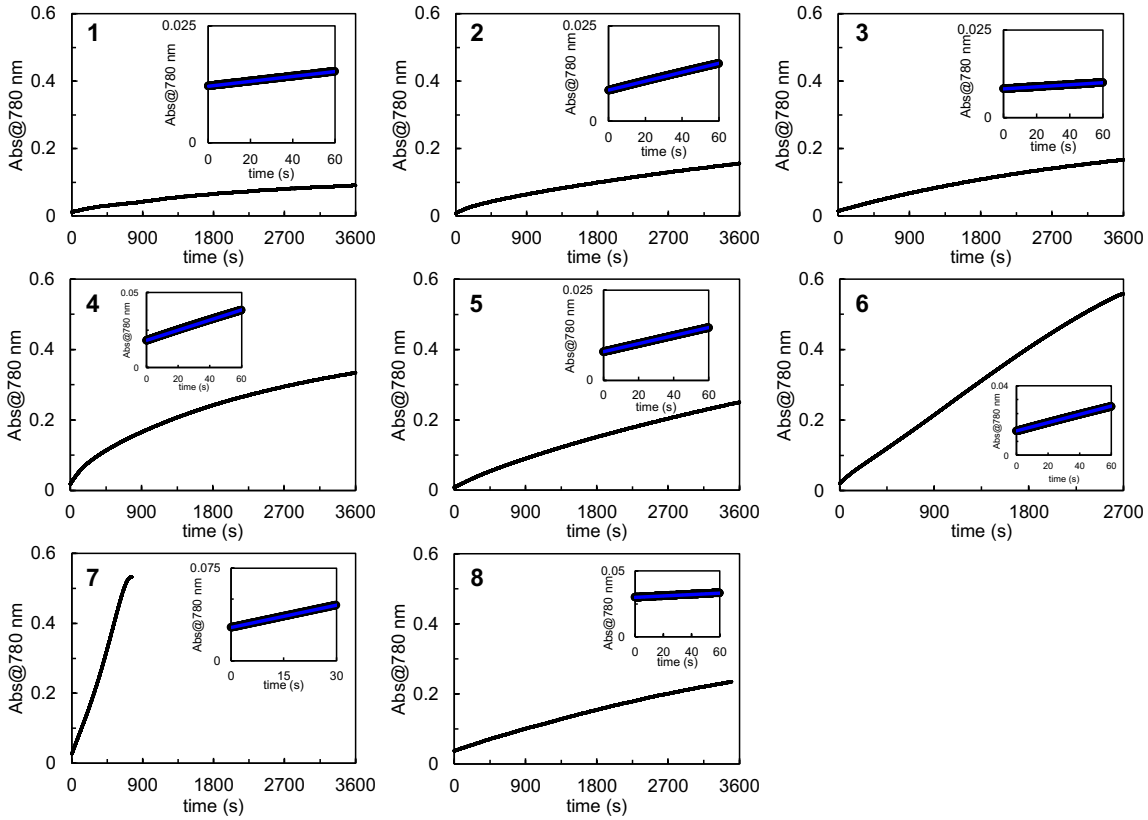

Figure S7. UV-visible time-course data for O_2 reduction catalyzed by complexes **1–8** that provide the basis for the TOFs associated with the complexes in Figure 3 of the main manuscript. Black trace: the O_2 reduction catalyzed by complexes **1–8**, which are obtained by subtracting the grey trace from the blue trace in Figure S4a. Concentration of Co complexes **1–8** for each study: **1**, 10 μM; **2**, 10 μM; **3**, 1 μM; **4**, 10 μM; **5**, 2 μM; **6**, 2 μM; **7**, 2.5 μM; **8**, 0.01 μM. Insets: the data points are fitted with linear regression to calculate the initial rates.

Initial rates of O_2 reduction (mM/s) = initial rate of Δ[Fc*]/(2 × time)

Turnover frequency (TOF) for O_2 reduction (s^{-1}) = initial rate of O_2 reduction/[Co].

Table S4. A summary of turnover frequencies (TOF, s^{-1}) for the O_2 reduction catalyzed by **1–8**.[a]

Co(por)	1	2	3	4	5	6	7	8
TOF (s^{-1})	0.0052	0.012	0.015	0.034	0.056	0.12	0.24	7.5

[a] Buffered conditions: 10 mM each of $HClO_4$ and $[NBu_4][ClO_4]$.

VI. Selectivity of ORR catalyzed by 1–8

A. $Ti^{IV}(O)SO_4$ colorimetric assay for H_2O_2 Quantification.

The first method for H_2O_2 quantification used was a colorimetric assay using aqueous $Ti^{IV}(O)SO_4$, modified from a literature procedure.[13,14] A calibration curve was constructed by first preparing a series of 10 mL DMF solutions with various concentrations of urea·H_2O_2 (0.05, 0.10, 0.15, 0.20, and 0.25 mM). A 0.1 mL solution of $Ti^{IV}(O)SO_4$ was added to the above solutions, respectively. The absorbance at 407 nm was measured by UV-visible spectroscopy to create the calibration curve as shown in Figure S8.

To quantify H_2O_2 in the catalytic reaction mixture, a 0.5 mL aliquot of the catalytic reaction (cf. Section V) was vigorously mixed with 2 mL deionized H_2O and 5 mL dichloromethane. The aqueous layer (≈ 2.1 mL) was collected, and a 20 μL solution of $Ti^{IV}(O)SO_4$ was added to this aqueous layer. The absorbance at 407 nm was measured by UV-visible spectroscopy.

The absorbance at 407 nm was analyzed with (red trace) and without (black trace) $Ti^{IV}(O)SO_4$ (cf. Figure S9). The concentrations of H_2O_2 in different catalytic reaction mixtures were calculated from the slope of the calibration curve (cf. Figure S8a, y = 0.7415x + 0.0044) as follows:

1) ΔAbs = Abs@407 nm (Figure S9, red trace) – Abs@407 nm (Figure S9, black trace)

2) $[H_2O_2]_{exp}$ (mM) = (ΔAbs – 0.0044)/0.7415

3) For a $2e^-/2H^+$ catalytic O_2 reduction reaction (Fc* is 1 mM for all catalytic reactions):
$[H_2O_2]$ = 0.5 mM × (0.5 mL (aliquot)/2.1 mL (aqueous layer)) = 0.120 mM

4) Selectivity of H_2O_2 (%) = $[H_2O_2]_{exp}$/0.120 mM

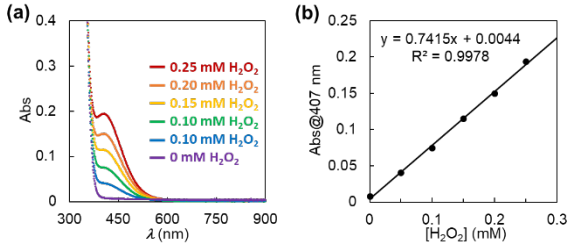

Figure S8. (a) UV-visible spectra for $Ti^{IV}(O)SO_4$-based detection of varying (0–0.25 mM) concentrations of H_2O_2. (b) Calibration curve constructed from data in Figure S8a.

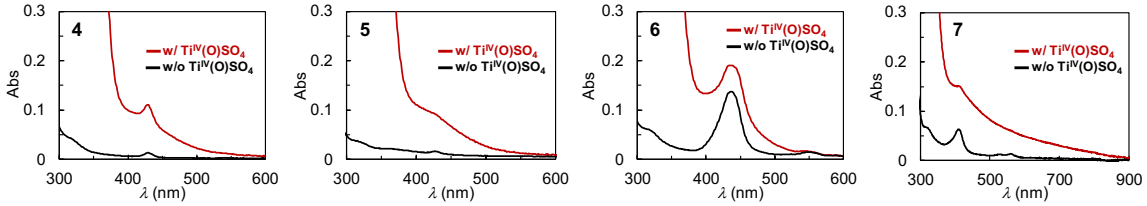

Figure S9. UV-visible spectra for the detection of H_2O_2 from O_2 reduction catalyzed with **4–7** via treatment with $Ti^{IV}(O)SO_4$ (red trace) and background spectra without adding $Ti^{IV}(O)SO4$. The selectivity for catalytic O_2 reduction by **4–7**: **4**, 95 %; **5**, 97 %; **6**, 95 %; **7**, 95%.

B. Iodometric titration for H_2O_2 quantification

The second method for quantitation of H_2O_2 produced was determined by titration with iodide ion, as described previously in the literature.[15,16] In an iodometric titration, the formation of I_3^- and the consumption of H_2O_2 follows a one-to-one ratio (2 NaI + $\mathbf{H_2O_2} \rightarrow I_2$ + 2 NaOH, NaI + $I_2 \rightarrow \mathbf{NaI_3}$). The concentration H_2O_2 can be derived from the concentration of I_3^- (Abs@361 nm = $\varepsilon b[I_3^-]$). All iodometric titrations are conducted anaerobically to avoid the oxidation of I^- to I_3^- by O_2.

To quantify H_2O_2 in the catalytic reaction mixture, a 60 μL aliquot of the 3 mL catalytic reaction mixture was diluted in CH_3CN (2.94 mL), and an excess amount of NaI (0.1 M) was then added. The amount of I_3^- formed was determined by the UV-visible absorption spectroscopy (λ_{max}@361 nm, $\varepsilon = 2.8 \times 10^4$ M^{-1} cm^{-1}).[15] The absorbance at 361 nm was compared from aliquots withdrawn and analyzed with and without added NaI (red and black traces, respectively, in Figure S10). The difference in the absorbance at 361 nm was used to quantify the amount of H_2O_2 formed in the catalytic reaction, according to the following considerations:

(1) For a $2e^-/2H^+$ catalytic O_2 reduction:

$$O_2 + 2\ Fc^*\ (1.0\ mM) + 2\ HA \xrightarrow{cat.\ [LCo]} H_2O_2\ (0.5\ mM) + 2\ Fc^{*+} + 2\ A^-$$

(2) The diluted CH_3CN solution of the product mixture contains the following theoretical amount of hydrogen peroxide: $[H_2O_2]$ (mM) = (60 μL/3000 μL) × 0.5 mM = 0.01 mM.

(3) Abs@361 nm (red trace, Fig. S10) – Abs@361 nm (black trace, Fig. S10) = $\varepsilon b[I_3^-]$, $[I_3^-] = [H_2O_2]_{exp}$

(4) Selectivity of H_2O_2 (%) = $[H_2O_2]_{exp}$/0.01 mM

Two control experiments were conducted:
NaI (0.1 M) and Fc^{*+} (1 mM) were combined in the presence of 10 mM each of $HClO_4$ and $[NBu_4][ClO_4]$ in DMF anaerobically. The mixture was analyzed by UV-visible spectroscopy (300-900 nm) anaerobically for 60 min. No reaction was observed (i.e., no change in the Fc^{*+} concentration in the absence of **6**).

NaI (0.1 M) was combined with catalytic amount of **6** (10 μM) in the presence of 10 mM each of $HClO_4$ and $[NBu_4][ClO_4]$ in DMF anaerobically. The mixture was analyzed by UV-visible spectroscopy (300-900 nm) anaerobically for 60 min, and no reaction was observed (i.e., no catalytic oxidation of I^- by **6**).

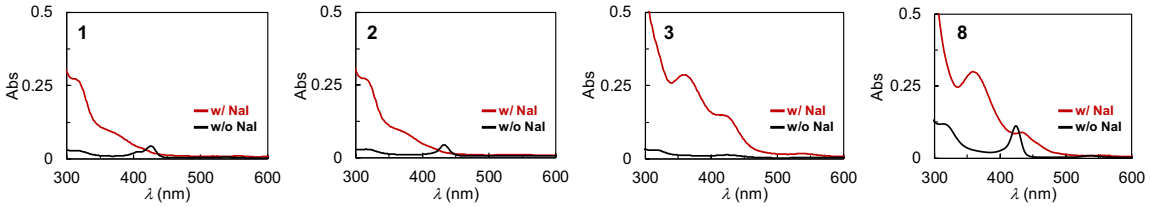

Figure S10. UV-Vis absorption spectral change before (black) and after (red) the addition of NaI (excess, 0.1 M) to a diluted reaction mixture in MeCN. The selectivity for catalytic O_2 reduction to H_2O by **1–3, 8**: **1**, 98 %; **2**, 93 %; **3**, 98 %; **8**, 97%.

Table S5. A summary of selectivity for O_2 reduction catalyzed by **1–8**

Co(por)	**1**	**2**	**3**	**4**	**5**	**6**	**7**	**8**
% H_2O_2	98 %	93 %	98 %	95 %	97 %	95 %	95 %	97 %

VII. Turnover frequencies and effective overpotentials for Co(por), Co(N_2O_2), and Fe(por)

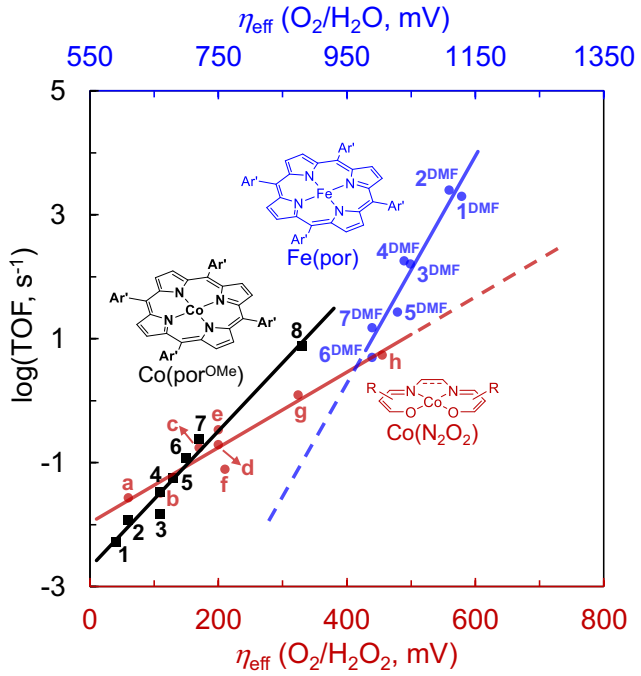

Figure S11. Linear free energy relationships that correlate log(TOF) and η_{eff} for the O_2 reduction to H_2O or H_2O_2, catalyzed by Co(por), Co(N_2O_2) (red),[17] and Fe(por) (blue).[18]

Chart S2. Molecular Co(N_2O_2) complexes **a–h** for catalytic O_2 reduction[17]

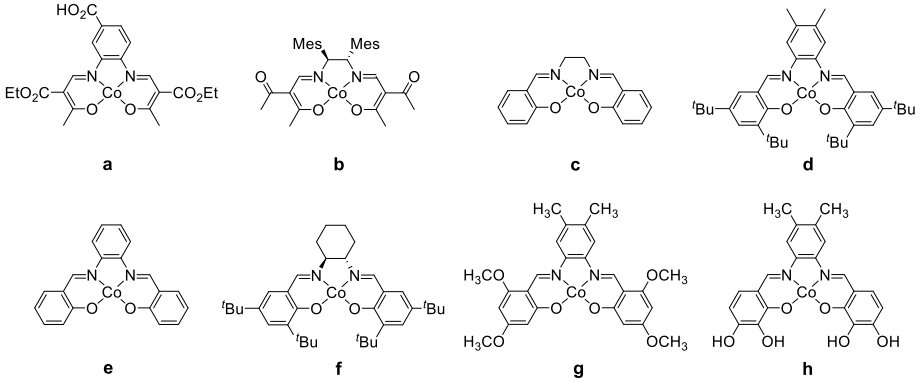

For the O_2 reduction catalyzed by Co(N_2O_2) complexes, the thermodynamic reduction potential of E_{O_2/H_2O_2} under standard state conditions (i.e., 1 M H_2O_2) is calculated to be 0.37 V versus $Fc^{*+/0}$, which is used to calculate the effective overpotentials of O_2 reduction catalyzed by **a**–**h** in this study.[17]

Chart S3. Molecular Fe(por) complexes for catalytic O_2 reduction[18]

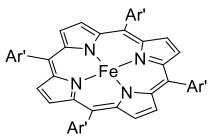

Ar' = Ph-2-CO_2H	1^{DMF}
Ar' = Ph-2-CO_2Me	2^{DMF}
Ar' = Ph-4-OMe	3^{DMF}
Ar' = Ph-4-SO_3H	4^{DMF}
Ar' = Ph	5^{DMF}
Ar' = Ph-4-Br	6^{DMF}
Ar' = Ph-4-CO_2H	7^{DMF}

For the O_2 reduction catalyzed by Fe(por) complexes, the thermodynamic reduction potential of E_{O_2/H_2O} under standard state conditions (i.e., 1 M H_2O) is calculated to be 0.50 V versus $Fc^{+/0}$ using the using the Nernst equation as below:

E_{O_2/H_2O} vs. $Fc^{+/0}$ (V) = 0.55 V – 0.030 V × log($[H_2O]_{1\ M}/[H_2O]_{20\ mM}$) = 0.50 V

This potential is used to calculate the effective overpotentials of O_2 reduction catalyzed by **1**^{DMF}–**7**^{DMF} in this study (i.e., Figures 2 and 5 in the main manuscript).[18]

Table S6. Turnover Frequencies (TOF, s^{-1}) and Effective Overpotentials (η_{eff}, V) of O_2 Reduction Catalyzed with Co(por), Co(N_2O_2), and Fe(por).

Co(por)[a]	TOF (s^{-1})	η_{eff} (V)[d]	Co(N_2O_2)[b]	TOF (s^{-1})	η_{eff} (V)[d]	Fe(por)[c]	TOF (s^{-1})	η_{eff} (V)[e]
1	0.0052	0.04	**a**	0.027	0.06	**1**^{DMF}	2000	1.13
2	0.012	0.06	**b**	0.032	0.11	**2**^{DMF}	2500	1.11
3	0.015	0.11	**c**	0.17	0.17	**3**^{DMF}	160	1.05
4	0.034	0.11	**d**	0.21	0.20	**4**^{DMF}	180	1.04
5	0.056	0.13	**e**	0.34	0.20	**5**^{DMF}	27	1.03
6	0.12	0.15	**f**	0.079	0.21	**6**^{DMF}	5	0.99
7	0.24	0.17	**g**	1.1	0.32	**7**^{DMF}	15	0.99
8	7.5	0.33	**h**	5.5	0.46			

[a]This study. [b]See ref. 17 for experimental details. [c]See ref. 18 for experimental details. [d]The effective overpotentials were calculated assuming standard state conditions (i.e., 1 M H_2O_2). [e]The effective overpotentials were calculated assuming standard state conditions (i.e., 1 M H_2O).

VIII. Turnover frequencies of previous O_2 reduction studies

A. Calculation of turnover frequencies for chemical O_2 reduction

For the chemical reduction of O_2 reactions studied by UV-vis spectroscopy, the TOFs are calculated in the same manner as the Section V. Initial rates, in units of $mM \cdot s^{-1}$, were obtained by fitting UV-visible time-course data with linear regression during the first ~5% of the reaction for each of original reference. The turnover frequencies (TOFs, s^{-1}) were then determined by dividing the number of electron transferred to account for the conversion of O_2 to H_2O_2 on the basis of consumption of single-electron reductant (ferrocene derivatives) and the catalyst concentration (TOF (s^{-1}) = $\frac{\Delta[Fc^*]/2}{[Co]\times time}$, see also Section V).[2-6,19]

Table S7. A summary of turnover frequencies for previous chemical O_2 reduction studies

Co	Initial time for estimating TOF	TOF (s^{-1})[a]	Rate Law	Reference
Co(TPP)	4.2 ms	4500	k[Co][Fc]	2 (Fig. 2 in ref. 2)
Co(OEP)	0.5 s	170	k[Co][Fc]	3, 4 (Fig. 1a in ref. 3)
Co(Ph_8Pc)	50 s	0.5 (Me_2Fc)	k[Co][H^+][O_2]	19 (Fig. S7 in ref. 19)
Co(Ch_1)	83 s	250	k[Co][H^+][O_2]	5, 6 (Fig. S6 in ref. 6)
Co(Ch_2)	55 s	380	k[Co][H^+][O_2]	6 (Fig. S6 in ref. 6)
Co(Ch_3)	17 s	1200	k[Co][H^+][O_2]	6 (Fig. S6 in ref. 6)

[a]TOFs were calculated based on the initial consumption of ferrocene derivatives by catalyst concentration per second (TOF (s^{-1}) = $-1/2 \times$ [Fc']/([Co] $\times$ time)).

B. Calculation of turnover frequencies for electrochemical O_2 reduction

1. For the electrochemical reduction of O_2 reactions studied by cyclic voltammetry (CV), the TOFs (k_{obs}s, s^{-1}) are calculated according to eq S1. In equation S1, i_c is the catalytic current in the presence of catalysis, i_p is the catalytic current in the absence of catalysis, n_c (2) is the number of electrons transferred in the catalytic wave, n_p (1) is the number of electrons transferred in the non-catalytic wave, F is Faraday's constant (F = 96500 C mol^{-1}), ν is the scan rate in V/s^{-1}.[20-28]

$$\frac{i_c}{i_p} = \frac{n_c}{0.447 n_p^{3/2}} \sqrt{\frac{RT\boldsymbol{k_{obs}}}{Fv}} \qquad \text{(eq S1)}$$

2. For the electrochemical reduction of O_2 reactions studied by rotating disk electrochemistry (RDE), the TOFs (k_{obs}s, s^{-1}) are calculated according to eq S2. In equation S2, i_{pl} is the catalytic plateau current, n_c (2) is the number of electrons transferred in the catalytic wave, F is Faraday's constant (F = 96500 C mol^{-1}), A is the surface area of the disk electrode, C°_{cat} is the catalyst concentration, D_{cat} is the diffusion constant of the catalyst.[20-28]

$$i_{pl} = n_c F A C^{\circ}_{cat} \sqrt{D_{cat}\boldsymbol{k_{obs}}} \qquad \text{(eq S2)}$$

Table S8. A summary of turnover frequencies for previous electrochemical O_2 reduction studies

Co	i_c (μA)[a]	i_p (μA)[b]	Technique	TOF (s^{-1})	Reference
Co([14]aneN$_4$)	475[c]	–	RDE	2.5	29 (Fig. 3 in ref. 29)
Co(TMPyMeP)	64	2	CV	36	30 (Fig. 5 in ref. 30)
Co(hmc)	33	19	CV	0.29	31 (Fig. 7 in ref. 31)
Co(Br$_8$TMPyMeP)	35	2	CV	59 (pH 1.2)	32 (Figs. 2, 3 in ref. 32)
Co(Br$_8$TMPyMeP)	30	2	CV	44 (pH 7)	32 (Figs. 2, 3 in ref. 32)
Co(Br$_8$TPPS)	21	2	CV	21	33 (Figs. 2, 3 in ref. 33)
Co(TMPyP)	68	10	CV	4.5	34 (Figs. 2c, 5 in ref. 34)

[a] i_c: catalytic current. [b] i_p: non-catalytic current. [c] i_{pl}: catalytic plateau current.

3. The TOF of Co(TMPyMeP) was estimated using the CVs presented in Ref. 30, Figure 5. The catalytic CV does not exhibit ideal S-shaped electrocatalytic behavior with a plateau (the current is limited by diffusion). Therefore, the calculated catalytic TOF represents a lower limit. The i_c and i_p were estimated to be 64 μA and 2 μA, respectively, according to the scale bar in Figure S12. The turnover frequency was therefore calculated to be 36 s^{-1} using the equation S1.

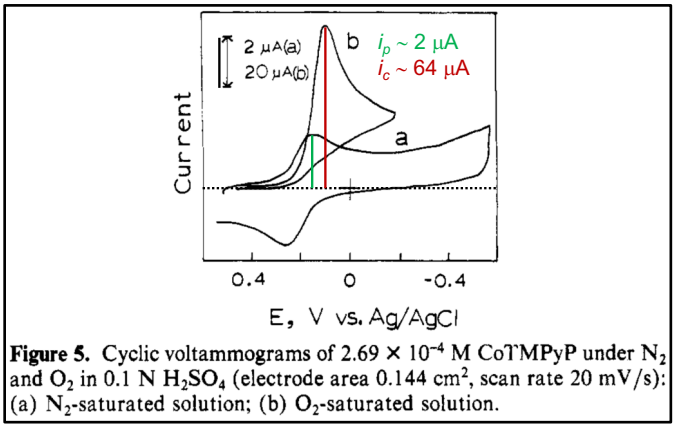

Figure 5. Cyclic voltammograms of 2.69 × 10^{-4} M CoTMPyP under N_2 and O_2 in 0.1 N H_2SO_4 (electrode area 0.144 cm^2, scan rate 20 mV/s): (a) N_2-saturated solution; (b) O_2-saturated solution.

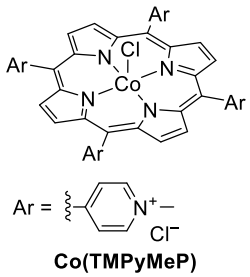

Co(TMPyMeP)

Figure S12. The cyclic voltammograms used to estimate the TOF of electrochemical O_2 reduction catalyzed by Co(TMPyMeP). Figure S12 is reproduced from Figure 5 of ref. 30; copyright 1985 American Chemical Society.)

4. The TOF of Co([14]aneN$_4$) was estimated using the rotating disk voltammogram (RDV) presented in Ref. 29, Figure 3. The i_{pl} was estimated to be 475 μA according to the scale bar in Figure S13. The turnover frequency was therefore calculated to be 2.5 s^{-1} using the equation S2.

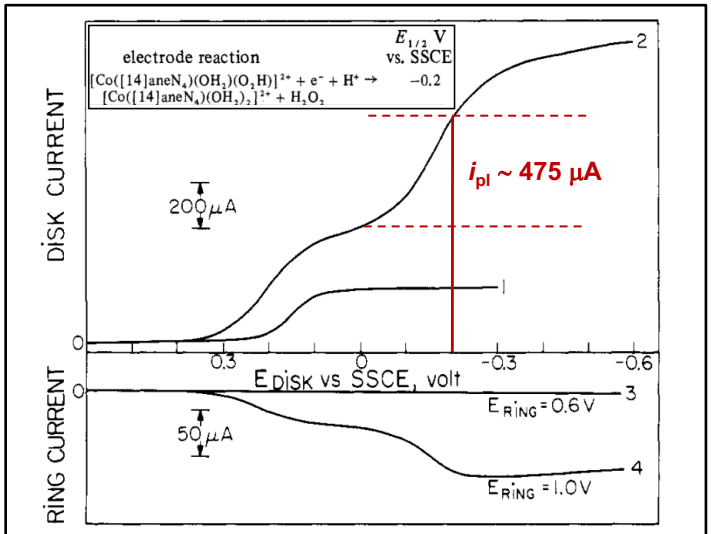

Figure 3. Ring–disk current–potential curves for 1.5 mM [Co([14]-aneN$_4$)(OH$_2$)$_2$]$^{3+}$ in 0.5 M HClO$_4$ at a rotation rate of 900 rpm. (Curve 1) Disk current in the absence of dioxygen. (Curve 2) Disk current in dioxygen-saturated solution. (Curve 3) Ring current vs. disk potential in dioxygen-saturated solution with ring potential at 0.6 V. (Curve 4) As in 3 except ring potential is at 1.0 V.

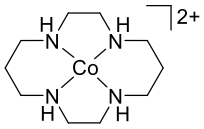

Co([14]aneN$_4$)

Figure S13. The RDV used to estimate the TOF of electrochemical O_2 reduction catalyzed by Co([14]aneN$_4$). Figure S13 is reproduced from Figure 3 in ref. 29; copyright 1981 American Chemical Society.)

IX. Effective overpotentials of previous O_2 reduction studies

A. Estimation of effective overpotentials for chemical O_2 reduction

For the O_2 reduction conducted in organic solutions, the thermodynamic reduction potentials of O_2/H_2O_2 were initially estimated via the OCP measurements of E_{H^+/H_2} (Sections I-II). The background concentration of H_2O_2 is assumed to be at standard state condition (i.e., 1 M) for each reaction due to the lack of adding known amount of H_2O_2 for the previous O_2 reduction studies This assumption is necessary to estimate the effective overpotential and provide the basis to construct the liner free energy relationship between the log(TOF) and the η_{eff} (cf. Figure 6 in the main manuscript).

Table S9. A summary of effective overpotentials for previous chemical O_2 reduction studies

Co	$E_{1/2}(Co^{III/II})$, mV[a]	$E(O_2/H_2O_2)$, mV[a]	$\eta_{eff}(O_2/H_2O_2)$, mV[a,b]	Reference
Co(TPP)	430	990	560	2 (Table I in ref. 2)
Co(OEP)	390	970	580	3, 4 (Fig. 4 in ref. 3)
$Co(Ph_8Pc)$	580	*[c]	*[c]	19 (Scheme 3 in ref. 19)
$Co(Ch_1)$	560	990	430	5, 6 (Fig. 4 in ref. 6)
$Co(Ch_2)$	530	990	460	6 (Fig. 4 in ref. 6)
$Co(Ch_3)$	480	990	510	6 (Fig. 4 in ref. 6)

[a]All half-wave potentials of Co catalysts ($E_{1/2}(Co^{III/II})$) and reduction potentials of O_2/H_2O_2 ($E(O_2/H_2O_2)$) are relative to $Fc^{*+/0}$. [b]All thermodynamic reduction potentials of O_2/H_2O_2 vs. $Fc^{*+/0}$ were estimated via the OCP measurements. The background concentration of H_2O_2 was assumed at standard-state conditions of 1 M for all studies to estimate η_{eff}. [c]Estimation of E_{O_2/H_2O_2} from OCP measurement of E_{H^+/H_2} was not possible because the reaction was conducted under non-buffered conditions.[1]

B. Estimation of effective overpotentials for electrochemical O_2 reduction

For the O_2 reduction conducted in aqueous solutions, the thermodynamic reduction potentials of O_2/H_2O_2 were calculated using the Nernst equation (cf. eq S3). The background concentration of H_2O_2 is assumed to be at standard state condition (1 M) for each reaction due to the lack of adding known amount of H_2O_2 for the previous O_2 reduction studies. This assumption is necessary to estimate the effective overpotential and provide the basis to construct the liner free energy relationship between the log(TOF) and the η_{eff} (cf. Figure 5 in the main manuscript).

$$E_{O_2/H_2O_{2(aq)}} \text{ vs. NHE} = 0.68\ \text{V} - 0.059\ \text{V} \times \text{pH} \qquad \text{(eq S3)}$$

Table S10. A summary of effective overpotentials for previous electrochemical O_2 reduction studies

Co	pH value	$E_{1/2}$, mV[a]	$E(O_2/H_2O_2)$, mV[a]	$\eta_{eff}(O_2/H_2O_2)$, mV[a,b]	Reference
Co([14]aneN_4)	0.3	400[d]	660	260	29 (Fig. 1 in ref. 29)
Co(TMPyMeP)	1.2	420[d]	610	190	30 (Figs. 1, 5 in ref. 30)
Co(hmc)	2.9	360[d]	510	150	31 (Fig. 7 in ref. 31)
Co(Br_8TMPyMeP)	1.2	–56[e]	610	666	32 (Figs. 2, 3 in ref. 32)
Co(Br_8TMPyMeP)	7.0	–66[e]	267	333	32 (Figs. 2, 3 in ref. 32)
Co(Br_8TPPS)	8.9	–390[e]	155	545	33 (Figs. 2, 3 in ref. 33)
Co(TMPyP)	1.0	350[d]	620	270	34 (Figs. 2c, 5 in ref. 34)

[a]All half-wave potentials of Co catalysts ($E_{1/2}$) and reduction potentials of O_2/H_2O_2 ($E(O_2/H_2O_2)$) are relative to NHE. [b]All thermodynamic reduction potentials of O_2/H_2O_2 vs. NHE were estimated via the Nernst equation: $E(O_2/H_2O_2)$ = 0.68 V – 0.059 V × pH. The background concentration of H_2O_2 was assumed at standard-state conditions of 1 M for all studies to estimate $\eta_{eff.}$ [d]Half-wave potentials of the Co^{III}/Co^{II} redox couple. [e]Half-wave potentials of the Co^{II}/Co^{I} redox couple.

X. Relationship between log(TOF) and $E_{1/2}$(Co)

Relationship between the logarithm of turnover frequency, log(TOF), and the half-wave potential of cobalt complexes, $E_{1/2}$(Co) is presented in Figure S12. The log(TOF) and $E_{1/2}$(Co) values were taken from the Sections VIII and IX, respectively.

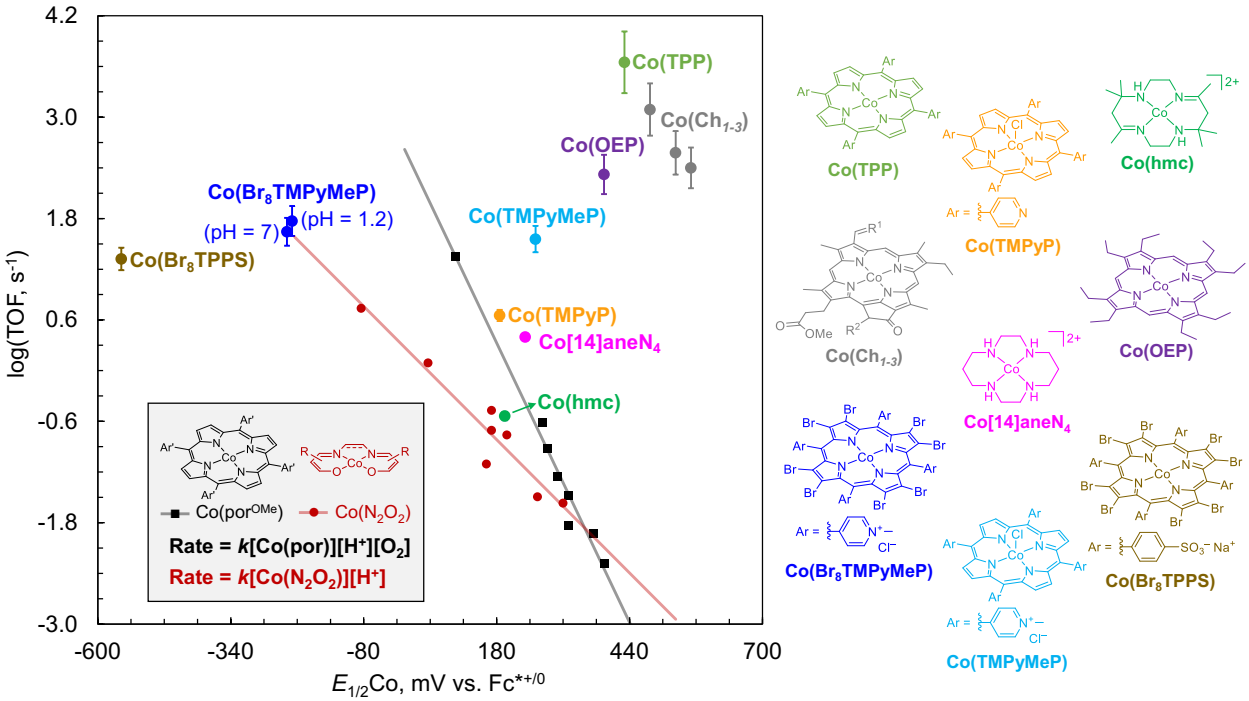

Figure S14. Dependence of log(TOF) versus $E_{1/2}$(Co) for $2e^-/2H^+$ reduction of O_2 to H_2O_2. The Co(por) data (black trace) is from this study, and the $Co(N_2O_2)$ data (red trace) was taken from Figure 5 in ref. 17 The error bar for log(TOF) is estimated to be about ± 5%.

XI. References

1. Roberts, J. A. S.; Bullock, R. M. Direct Determination of Equilibrium Potentials for Hydrogen Oxidation/Production by Open Circuit Potential Measurements in Acetonitrile. *Inorg. Chem.* **2013,** *52*, 3823-3835.
2. Fukuzumi, S.; Mochizuki, S.; Tanaka, T. Efficient Reduction of Dioxygen with Ferrocene Derivatives, Catalyzed by Metalloporphyrins in the Presence of Perchloric Acid. *Inorg. Chem.* **1989,** *28*, 2459-2465.
3. Fukuzumi, S.; Okamoto, K.; Gros, C. P.; Guilard, R. Mechanism of Four-Electron Reduction of Dioxygen to Water by Ferrocene Derivatives in the Presence of Perchloric Acid in Benzonitrile, Catalyzed by Cofacial Dicobalt Porphyrins. *J. Am. Chem. Soc.* **2004,** *126*, 10441-10449.
4. Fukuzumi, S. Metal Ion-Coupled Electron-Transfer Reduction of Dioxygen. *Chem. Lett.* **2008,** *37*, 808-813.
5. Mase, K.; Ohkubo, K.; Fukuzumi, S. Efficient Two-Electron Reduction of Dioxygen to Hydrogen Peroxide with One-Electron Reductants with a Small Overpotential Catalyzed by a Cobalt Chlorin Complex. *J. Am. Chem. Soc.* **2013,** *135*, 2800-2808.
6. Mase, K.; Ohkubo, K.; Fukuzumi, S. Much Enhanced Catalytic Reactivity of Cobalt Chlorin Derivatives on Two-Electron Reduction of Dioxygen to Produce Hydrogen Peroxide. *Inorg. Chem.* **2015,** *54*, 1808-1815.
7. Pegis, M. L.; Roberts, J. A. S.; Wasylenko, D. J.; Mader, E. A.; Appel, A. M.; Mayer, J. M. Standard Reduction Potentials for Oxygen and Carbon Dioxide Couples in Acetonitrile and *N*,*N*-Dimethylformamide. *Inorg. Chem.* **2015,** *54*, 11883-11888.
8. Marenich, A. V.; Cramer, C. J.; Truhlar, D. G. Universal Solvation Model Based on Solute Electron Density and on a Continuum Model of the Solvent Defined by the Bulk Dielectric Constant and Atomic Surface Tensions. *J. Phys. Chem. B* **2009,** *113*, 6378-6396.
9. Marenich, A. V.; Kelly, C. P.; Thompson, J. D.; Hawkins, G. D.; Chambers, C. C.; Giesen, D. J.; Winget, P.; Cramer, C. J.; Truhlar, D. G., *Minnesota Solvation Database – version 2012*. University of Minnesota: Minneapolis, 2012.
10. Wang, Y.-H.; Schneider, P. E.; Goldsmith, Z. K.; Mondal, B.; Hammes-Schiffer, S.; Stahl, S. S. Brønsted Acid Scaling Relationships Enable Control Over Product Selectivity from O_2 Reduction with a Mononuclear Cobalt Porphyrin Catalyst. *ACS Cent. Sci.* **2019,** *5,* 1024-1034.
11. Sato, T.; Hamada, Y.; Sumikawa, M.; Araki, S.; Yamamoto, H. Solubility of Oxygen in Organic Solvents and Calculation of the Hansen Solubility Parameters of Oxygen. *Ind. Eng. Chem. Res.* **2014,** *53*, 19331-19337.
12. Su, B.; Hatay, I.; Ge, P. Y.; Mendez, M.; Corminboeuf, C.; Samec, Z.; Ersoz, M.; Girault, H. H. Oxygen and Proton Reduction by Decamethylferrocene in Non-Aqueous Acidic Media**.** *Chem. Commun.* **2010,** *46,* 2918-2919.
13. (a) Lee, Y.; Park, G. Y.; Lucas, H. R.; Vajda, P. L.; Kamaraj, K.; Vance, M. A.; Milligan, A. E.; Woertink, J. S.; Siegler, M. A.; Narducci Sarjeant, A. A.; Zakharov, L. N.; Rheingold, A. L.; Solomon, E. I.; Karlin, K. D. Copper(I)/O_2 Chemistry with Imidazole Containing Tripodal Tetradentate Ligands Leading to μ-1,2-Peroxo−Dicopper(II) Species. *Inorg. Chem.* **2009,** *48*, 11297-11309.
14. Anson, C. W.; Stahl, S. S. Cooperative Electrocatalytic O_2 Reduction Involving Co(salophen) with *p*-Hydroquinone as an Electron–Proton Transfer Mediator. *J. Am. Chem. Soc.* **2017,** *139*, 18472-18475.
15. Mair, R. D.; Graupner, A. J. Determination of Organic Peroxides by Iodine Liberation Procedures. *Anal. Chem.* **1964,** *36*, 194-204.
16. Fukuzumi, S.; Kuroda, S.; Tanaka, T. Flavin Analog-metal Ion Complexes Acting as Efficient Photocatalysts in the Oxidation of *p*-Methylbenzyl Alcohol by Oxygen under Irradiation with Visible Light. *J. Am. Chem. Soc.* **1985,** *107*, 3020-3027.
17. Wang, Y.-H.; Pegis, M. L.; Mayer, J. M.; Stahl, S. S. Molecular Cobalt Catalysts for O_2 Reduction: Low-Overpotential Production of H_2O_2 and Comparison with Iron-Based Catalysts. *J. Am. Chem. Soc.* **2017,** *139*, 16458-16461.

18. Pegis, M. L.; McKeown, B. A.; Kumar, N.; Lang, K.; Wasylenko, D. J.; Zhang, X. P.; Raugei, S.; Mayer, J. M. Homogenous Electrocatalytic Oxygen Reduction Rates Correlate with Reaction Overpotential in Acidic Organic Solutions. *ACS Cent. Sci.* **2016,** *2,* 850-856.
19. Honda, T.; Kojima, T.; Fukuzumi, S. Proton-Coupled Electron-Transfer Reduction of Dioxygen Catalyzed by a Saddle-Distorted Cobalt Phthalocyanine. *J. Am. Chem. Soc.* **2012,** *134*, 4196-4206.
20. For calculation of turnover frequencies in molecular electrocatalysis studies (i.e., cyclic voltammetry, rotating disk electrochemistry), see the following and refs. 2120–28: Nicholson, R. S.; Shain, I. Theory of Stationary Electrode Polarography. Single Scan and Cyclic Methods Applied to Reversible, Irreversible, and Kinetic Systems. *Anal. Chem.* **1964,** *36*, 706-723.
21. Saveant, J. M.; Vianello, E. Potential-sweep Chronoamperometry: Kinetic Currents for First-order Chemical Reaction Parallel to Electron-transfer Process (Catalytic Currents). *Electrochim. Acta* **1965,** *10*, 905-920.
22. Nicholson, R. S.; Shain, I. Theory of Stationary Electrode Polarography for a Chemical Reaction Coupled between Two Charge Transfers. *Anal. Chem.* **1965,** *37*, 178-190.
23. Savéant, J. M.; Vianello, E. Potential-sweep Voltammetry: General Theory of Chemical Polarization. *Electrochim. Acta* **1967,** *12*, 629-646.
24. Andrieux, C. P.; Dumas-Bouchiat, J. M.; Savéant, J. M. Homogeneous Redox Catalysis of Electrochemical Reactions: Part IV. Kinetic Controls in the Homogeneous Process as Characterized by Stationary and Quasi-stationary Electrochemical Techniques. *J. Electroanal. Chem.* **1980,** *113*, 1-18.
25. Bard, A. J.; Faulkner, L. R. *Electrochemical Methods: Fundamentals and Applications.* Wiley: New Jersey, 2001, pp 331-364.
26. Savéant, J.-M. Molecular Catalysis of Electrochemical Reactions. Mechanistic Aspects. *Chem. Rev.* **2008,** *108*, 2348-2378.
27. Rountree, E. S.; McCarthy, B. D.; Eisenhart, T. T.; Dempsey, J. L. Evaluation of Homogeneous Electrocatalysts by Cyclic Voltammetry. *Inorg. Chem.* **2014,** *53*, 9983-10002.
28. Costentin, C.; Passard, G.; Savéant, J.-M. Benchmarking of Homogeneous Electrocatalysts: Overpotential, Turnover Frequency, Limiting Turnover Number. *J. Am. Chem. Soc.* **2015,** *137*, 5461-5467.
29. Geiger, T.; Anson, F. C. Homogeneous Catalysis of the Electrochemical Reduction of Dioxygen by a Macrocyclic Cobalt(III) Complex. *J. Am. Chem. Soc.* **1981,** *103*, 7489-7496.
30. Chan, R. J. H.; Su, Y. O.; Kuwana, T. Electrocatalysis of Oxygen Reduction. 5. Oxygen to Hydrogen Peroxide Conversion by Cobalt(II) Tetrakis(N-Methyl-4-Pyridyl)Porphyrin. *Inorg. Chem.* **1985,** *24*, 3777-3784.
31. Kang, C.; Anson, F. C. Effects of Coordination to a Macrocyclic Cobalt Complex on the Electrochemistry of Dioxygen, Superoxide, and Hydroperoxide. *Inorg. Chem.* **1995,** *34*, 2771-2780.
32. D'Souza, F.; Deviprasad, R. G.; Hsieh, Y.-Y. Synthesis and Studies on the Electrocatalytic Reduction of Molecular Oxygen by Non-planar Cobalt(II) Tetrakis-(N-methylpyridyl)-β-Octabromoporphyrin. *J. Electroanal. Chem.* **1996,** *411*, 167-171.
33. D'Souza, F.; Hsieh, Y.-Y.; Deviprasad, G. R. Electrocatalytic Reduction of Molecular Oxygen using Non-planar Cobalt Tetrakis-(4-Sulfonatophenyl)-β-Octabromoporphyrin. *J. Electroanal. Chem.* **1997,** *426*, 17-21.
34. He, Q.; Mugadza, T.; Hwang, G. S.; Nyokong, T. Mechanisms of Electrocatalysis of Oxygen Reduction by Metal Porphyrins in Trifluoromethane Sulfonic Acid Solution. *Int. J. Electrochem. Sci.* **2012,** *7,* 7045-7064.